

125

FACILITY FORM 602

N64-28077	(THRU)
(ACCESSION NUMBER)	none
26	(CODE)
(PAGES)	24
(NASA CR OR TMX OR AD NUMBER)	(CATEGORY)

RESEARCH ON A ONE-INCH-SQUARE LINEAR D-C PLASMA ACCELERATOR

by

A. F. CARTER, G. P. WOOD, D. R. McFARLAND  
and  
W. R. WEAVER  
National Aeronautics and Space Administration  
Langley Research Center  
Hampton, Virginia

AIAA Paper  
No. 64-699

# AIAA FOURTH ELECTRIC PROPULSION CONFERENCE

PHILADELPHIA, PENN.

AUGUST 31-SEPTEMBER 2, 1964

First publication rights reserved by American Institute of Aeronautics and Astronautics, 1290 Avenue of the Americas, New York, N. Y. 10019. Abstracts may be published without permission if credit is given to author and to AIAA. (Price — AIAA Member 50¢, Non-Member \$1.00).

**CASE FILE COPY**

# RESEARCH ON A 1-INCH-SQUARE LINEAR D-C PLASMA ACCELERATOR

By A. F. Carter\*, G. P. Wood\*\*, D. R. McFarland\*,  
and W. R. Weaver\*  
NASA Langley Research Center

## ABSTRACT

28077  
Some recent results from a continuing research program on plasma accelerators are reported for an accelerator that has a channel 1 inch square and 12 inches long. This accelerator uses nitrogen seeded with 0.3-percent mole fraction cesium and operates at relatively high-pressure, 50 mm Hg, and high magnetic field, 11,500 gauss. Power input to the accelerator is about 360 kw with about 50 amperes through each of 24 electrode pairs. The 1200-volt axial potential difference that is self-generated in the plasma between the ends of the accelerator has posed operational problems. This high voltage tends to find closed circuits to ground and back through many paths. Steps taken to alleviate these problems are described. Another problem is the erosion of the trailing edges of anodes and adjacent insulators because of the concentration of currents there due to large values of  $\omega r$ . Experience with this effect is described. Time-of-flight velocity measurements were made with injected spark and image-converter framing camera. Velocity at entrance is 6500 ft/sec and at exit 20,000 ft/sec and exit density is  $10^{-4}$  lb/ft<sup>3</sup>.

*Author*

## 1. INTRODUCTION

The research program on d-c linear crossed-field plasma accelerators conducted at the Langley Research Center is continuing. The primary objective of this program is to develop a high-speed facility capable of reentry testing; nevertheless, a report on the research at a conference on electric propulsion is deemed to be appropriate because the problems involved in developing an electric propulsion system or a high-speed test facility are essentially the same at this stage of development. This paper describes the progress made with the accelerator currently used at Langley.

## 2. 1-INCH-SQUARE ACCELERATOR TEST FACILITY

A photograph of the test facility is shown in figure 1. The arc heater is shown at the left of the picture. The accelerator is mounted in the large stainless-steel test chamber which is connected to a two-stage steam-ejector pump not shown in the photograph. Recording oscillographs are available for recording data. However, all currents in the accelerator are measured by using ammeters which are photographed by movie cameras. This was necessary because

---

\*Aerospace Engineer.

\*\*Head, Magnetohydrodynamics Section.

of high-voltage problems discussed in section 4. Four motor-generator sets in parallel capable of supplying 4000 amperes at 600 volts are available to power the arc heater. The accelerator is powered by batteries, each set of electrodes having its own separate supply.

### 3. ARC HEATER

The arc heater is an NASA design that was modified for use in this facility. A schematic is shown in figure 2. The water-cooled electrodes are axially symmetric, the outer one being the cathode and the inner one the anode. This arc heater does not give enthalpies high enough for the accelerator to operate without seeding. It was felt that seeding along the axis through the inner electrode would give better mixing than seeding through the sidewall; therefore, provision for seeding was made through the inner electrode as shown in figure 2. A large solenoid is used around the arc heater to spin the discharge. In the initial efforts to operate the arc heater, the discharge was very unstable and tended to be blown out by the aerodynamic force of the gas flow. The idea occurred to reverse the current in one of the pancakes making up the solenoid to get a magnetic field distribution as shown in figure 2. It was hoped that a force equal and opposite in direction to the aerodynamic force would be generated from the operation of the arc in the gradient of a magnetic field. After this was done, the arc operated in a stable position, indicating that a balance of forces had been achieved.

When attempts were made to operate the arc with seeding, more difficulties were experienced. When cesium vapor came into the arc jet, the arc voltage would drop from the normal operating value of 180 volts to approximately 50 volts. Since the amperage is limited to about 2500 amperes by the electrode design, this causes a severe drop in power. Also, electrical breakdown to the end of the seeding tube was frequently experienced. These two problems were cured by a combination of three things. First, the seeding rate was reduced from 2 percent to 0.3 of 1 percent. A flow of 0.2 gram per second of nitrogen gas was introduced around the seeding tube in the space between it and the inner electrode. (This is only about 3 percent of the total nitrogen flow rate.) Also, all silver-soldered joints were eliminated on the end of the inner electrode in the vicinity of the seeding tube and replaced by copper weld joints. The arc heater then operated satisfactorily with seeding, but some additional work was necessary on the seeding tube itself. A 0.125-inch O.D., 0.062-inch I.D., stainless-steel tube 60 inches long is used to vaporize the cesium. This tube, including the tip, must be maintained at a temperature greater than the boiling point of cesium or condensation will occur and the cesium will go into the arc jet in spurts. A stainless-steel tip was first used but it was found that radiation from the hot plasma in the arc jet would melt it. In the limited space available, water cooling of the tip to maintain its temperature between the boiling point of cesium and the melting point of the stainless steel was attempted, but the temperature difference was found to be too small to accomplish this satisfactorily. Molybdenum was then used in place of the stainless steel and melting of the tip was thus prevented. Satisfactory operation of the arc heater and the seeding tube together was then achieved. A drawing of the seeding tube is shown in figure 3.

#### 4. ACCELERATOR

The accelerator has a channel 1 inch by 1 inch in cross section (constant area) and is 12 inches long. The electrodes extend 0.285 inch in the axial direction and are separated by insulators of 0.160 inch. Both electrodes have a width of 1.75 inches, of which 1 inch is exposed to the plasma. The anodes are pure tungsten of 1/16-inch thickness which are backed by graphite. The cathodes are thoriated tungsten 1/16 inch thick and are backed by graphite at each end for a distance of 3/8 inch but not in the center 1-inch width. Hopefully this allows the cathodes to reach a higher operating temperature so that more electron emission will result. The insulators between the electrodes are boron nitride as are the sidewalls. A picture of the assembled accelerator is shown in figure 4. The accelerator is shown with one sidewall removed in figure 5.

Figure 6 shows a typical plot of the applied voltage and amperage distribution in the accelerator. The voltage was increased or decreased along the accelerator channel until approximately constant-current operation was achieved. The average current through each electrode is seen to be approximately 50 amperes, while the average voltage is about 300 volts. It can be seen from the voltage distribution plot that the applied voltage is slightly higher at the upstream end of the accelerator, levels off to a relatively constant value, and then drops at the downstream end. It might be assumed that, if  $\sigma$  is relatively constant, the sum  $j/\sigma + uxB$  would result in an increasing voltage from the upstream to the downstream end of the accelerator. A calculation was made of the sum  $j/\sigma + uxB$  at the upstream end of the accelerator using the following values for the run for which the data of figure 7, to follow, were obtained:

$$j = 1.6 \times 10^5 \text{ amps/m}^2$$

$$\sigma = 500 \text{ mhos/m}$$

$$u = 2000 \text{ m/s}$$

$$B = 1.14 \text{ webers/m}^2$$

This calculation gave a value of 67 volts. It appears that either sigma is rather low in the accelerator or the electrode sheath voltages are very high. Conclusions drawn from the measured axial potential in the accelerator help to determine which of the above conditions is prevailing. Figure 7 shows a plot of these potentials along the accelerator. These are the potentials developed by the plasma, as no  $E_x$  is applied to the electrodes. The value of  $E_x$  as determined from these measurements is 5100 volts per meter. A simple expression for  $E_x$  can be derived by writing Ohm's law for the current density in the axial direction and setting it equal to zero.

$$j_x = \sigma(E_x - u_{e,y}B_z) = 0$$

or

$$E_x = u_{e,y}B_z$$

and since

$$j_y \approx n_e e u_{e,y}$$

then

$$E_x \approx \frac{j_y B_z}{n_e e}$$

$j_y$ ,  $B$ , and  $E_x$  can be readily determined from measurements and therefore  $n_e$ , the number density of electrons can be obtained. With the above values, then,  $n_e = 2.3 \times 10^{20}$  electrons per cubic meter.

From the known mass flow rate and the seed mole fraction of original undissociated nitrogen, the number density of electrons can be determined. The values are:

$$\rho u = 10.4 \frac{\text{kgm}}{\text{m}^2 \cdot \text{sec}}$$

$$\alpha = 0.003$$

$$u = 2000 \text{ m/s}$$

$$m_{N_2} = 4.65 \times 10^{-26} \text{ kgm}$$

Therefore,  $n_e = \frac{\rho u \alpha}{m_{N_2}} = 3.3 \times 10^{20}$  electrons per cubic meter. This value of

$n_e$  is to be compared with the value obtained by using the measured value of  $E_x$  in the accelerator. There is always condensation of some of the cesium vapor in the arc-heater plenum and nozzle sections which may result in the calculated value of  $n_e$  being high.

A calculation of the value of the conductivity using the number density obtained from  $E_x$  gives

$$\sigma = 410 \text{ mhos/meter}$$

With this value of sigma, the voltage required across the channel at the accelerator entrance is

$$V = l(j/\sigma + uxB) = 67 \text{ volts}$$

and at the accelerator exit where the measured velocity is 6000 meter/sec. (See sec. 7.)

$$V = l(j/\sigma + uxB) = 167 \text{ volts}$$

The combined drop at the anode and cathode near the accelerator entrance is therefore approximately 230 volts and at the accelerator exit approximately 110 volts. These sheath voltages are higher than might be expected, but are not unreasonably high.

The axial potential developed in the accelerator created some troublesome problems during the efforts to make the accelerator operational. The 48 leads to the accelerator electrodes were fed through a metal plate (the lid to the test section) and ceramic-insulated terminals were soldered into it for electrical feedthroughs. When the accelerator was turned on, electrical breakdown occurred inside the test section at the lid where the current-carrying conductors came through it. Since the battery banks supplying power to the electrodes operate with no series resistance in the leads, only fuses, high short-circuit currents developed and damaged the terminals in the lid and the wiring before the fuses would burn out. Brass rods inserted through a dielectric lid were tried but the short circuits persisted. The problem was solved by bringing teflon-insulated wires through the dielectric cover of the test section without breaking the insulation until the wires were connected to the accelerator. A small O-ring was used around each wire to provide a leak-free seal.

Additional problems were experienced with the instrumentation. Three recorders used to record the test data were insulated for only 600 volts from galvanometer elements to the case, or ground. Burnout of the galvanometer elements and then arc-over to the case occurred at the elements which measured currents from electrical shunts in the leads to the upstream electrodes. The plasma at the downstream end of the accelerator grounds itself to the test section to form the return current path. The use of isolation transformers on the recorders helped somewhat, but breakdown still occurred between elements on the same recorder. Therefore, all currents were measured by using panel ammeters photographed by movie cameras, and two of the recorders were disconnected. The

high voltage then found its way to ground by breaking down in the meter that measures arc current on the control panel. This meter and the meter measuring arc voltage were then mounted on a large dielectric plate to insure complete isolation. By measuring all voltages and currents on panel-type meters photographed by movie cameras and by using the recorders to measure only temperatures and pressures, many successful tests were performed, with results from some of them being reported in this paper and some of them elsewhere (ref. 1).

Trouble was eventually experienced with the motor-generator sets that power the arc heater. Operation at 1200 to 1500 volts above ground potential was suspected to have caused the difficulty. The motor-generator sets could be grounded through a suitable resistance if the downstream end of the accelerator could be isolated so the potential there could go to 1200 to 1500 volts negative. It was felt that this was best accomplished by isolation of the test chamber from ground. A dielectric plate was inserted at the upstream support pedestal and a 20-inch-long section of dielectric pipe was inserted in the pipe leading from the test section to the vacuum pump. This failed to provide enough isolation, for breakdown to ground occurred in the gas flowing through the insulating pipe, allowing axial current flow in the accelerator. Steam was then sprayed into the pipe downstream of the test section to quench the ionization. This prohibited breakdown from occurring and testing then continued. The data in figure 7 were taken from a run after isolation of the test section was accomplished.

## 5. EROSION

The present 1-inch-square accelerator is not water cooled and therefore run times are limited due to the large power input into the accelerator. The limit on test time is approximately 3 seconds, for the tungsten electrodes quickly reach the melting point, especially the anodes, and cause severe eroding of the metal. A photograph of the anode wall using 1/16-inch-thick tungsten for the electrode is shown in figure 8. When 1/4-inch-thick tungsten is used for anodes, the melting is almost completely eliminated for the test time of approximately 3 seconds, as is shown in figure 9. Considerable erosion of the boron nitride sidewalls occurs, even though they are stored under vacuum and at temperatures of 250° F. However, a new grade of boron nitride is now available which appears to have an erosion resistance much superior to the former grade of material. The erosion is virtually eliminated if it is used within 4 to 6 weeks after being removed from moisture-proof containers and stored at atmospheric conditions. Figure 10 shows a photograph of used channel sidewalls made from boron nitride and from the new grade boron nitride used within the 4- to 6-week period. Use of the new boron nitride after this period again results in considerable spalling and loss of material. Therefore, storage under vacuum and temperatures of approximately 250° F may be helpful in reducing this erosion if long storage periods are contemplated.



## 6. DIAGNOSTICS

Since the 1-inch-square accelerator became operational the primary effort has been to develop a direct method of velocity measurement since this is the parameter of greatest interest. The early attempts to measure velocity were made at the exit of the nozzle of the arc heater to establish firmly the conditions existing there. The method consisted of creating a region of high luminosity by injecting a spark across the flow emerging from the nozzle and using two photomultiplier tubes located downstream of the injection point to detect the luminosity in the flow as it passed. A dual-beam oscilloscope recorded the passage of the luminous pulses. This method had the disadvantage that the isolation of the high voltage necessary to obtain a rather energetic spark was somewhat of a nuisance. Second, the luminosity from the spark had become rather diffuse by the time it reached the downstream photomultiplier and it was no longer sharply defined and was somewhat random. The first of these difficulties was overcome by proper selection of components but the second could never be completely satisfactorily overcome. Nevertheless, reasonably good measurements were obtained. The next step was to extend the technique to measuring velocities at the accelerator exit. It was felt that, instead of monitoring the motion of the spark luminosity with photomultiplier tubes, pictures of the spark could be taken as it moved downstream by using an image-converter camera. Measurement of the displacement over a given time interval could then be used to obtain the velocity. The camera used takes three frames in sequence, with variable exposure times and variable time between exposures. To increase the probability of obtaining usable data, the film holder was motorized and a series of six sequences were taken for each 3-second run, each sequence containing three frames. Figure 11 shows a series of four sequences with the accelerator on. The method of taking the pictures follows a set procedure. A motorized cam is used to actuate a switch six times, once every  $1/2$  second. The cam-driving motor is energized when the accelerator is turned on. Each time the switch closes, the mechanical shutter on the image converter camera is opened. The switch also starts a time-delay circuit which triggers the spark discharge through a triggered spark gap after the mechanical shutter has had time to open fully. The camera has an electronic shutter but use of the mechanical shutter is necessary because of the strong light intensity from the plasma and the fact that the electronic shutter has a transmission ratio as large as 1 to  $10^6$ . Just as much light would reach the film and fog it if the mechanical shutter were open for 0.2 of a second with the electronic shutter closed as reaches it during the 0.2 microsecond exposure with the electronic shutter. The mechanical shutter was set for  $1/25$  of a second and good pictures were obtained. The electronic shutter is actuated by a signal obtained by inductive coupling through a one-turn loop around one of the leads to the spark discharge. The three-frame sequence is then automatic.

One word of caution may be in order. Care must be taken that the current has decayed before the current path has swept downstream of the electrodes. Otherwise, the possibility of rail-type acceleration of the spark would exist. For the data presented in this paper, the current was damped to practically zero in less than 1 microsecond, or before the second frame was taken, by proper choice of voltage and capacitance and by inserting a 3-ohm damping resistance in series with the discharge.

Various values of voltage and capacitance were used in these experiments to arrive at a system giving good results. The following is a description of the spark discharge circuit that was finally used. A 50-kv, 0.02-microfarad capacitor was charged to approximately 30 kv. A 50-kv triggered spark gap and a 3-ohm damping resistance are included in the circuit. Teflon-insulated wires are fed through the dielectric lid of the test chamber without breaking the insulation. Small O-rings provide a leak-free seal. The two leads are soldered to a piece of 1/8-inch hard copper tubing and then an alumina tube is slipped over the copper tubing and extends up over the teflon insulation for approximately 3 inches. A 1/16-inch-diameter hole is drilled into the side of each alumina tube and into the copper. One-sixteenth-inch-diameter tungsten wires for the spark electrodes are then inserted into the holes and held in place with set screws threaded into the end of the copper tubing. This has worked very well in keeping the high-voltage spark from breaking down to undesired places. Since the test chamber was grounded during most of the experiments, it was also necessary to have the power supply secondary completely isolated from ground or else the discharge would tend to find paths to ground through the plasma downstream of the accelerator.

In addition to velocity measurements, a measure of the pitot pressure at the exit of the accelerator is made. The pitot tube is 0.375 inch in diameter and is constructed of water-cooled copper. Measurements of pitot pressure and observation of the shock wave at the front of the pitot tube are made with the end of the pitot tube about 0.25 inch from the exit of the accelerator. This was done to assure that the end of the pitot tube would be inside any expansion or shock waves formed at the exit. Observation of the shock wave for both accelerator on and off conditions can be used to verify that the flow is supersonic. The bow shock standoff distance from the end of the pitot tube is also observed. Figure 12 shows the shape and location of the bow shock at the pitot tube for the accelerator on and off conditions. The fact that the standoff distance decreases when the accelerator is turned on indicates an increase in the Mach number of the flow.

## 7. RESULTS

The conditions at the exit of the supersonic nozzle have been determined by a long series of experiments with the accelerator removed from the test section. Below is a list of representative values for the state of the gas:

$$\dot{m} = 6.68 \times 10^{-3} \text{ kg/s}$$

$$h = 6.2 \times 10^6 \text{ joules/kgm}$$

$$h_t = 8.2 \times 10^6 \text{ joules/kgm}$$

$$p = 6.9 \times 10^3 \text{ newtons/m}^2$$

$$u = 2.0 \times 10^3 \text{ m/s}$$

$$\rho = 5.2 \times 10^{-3} \text{ kgm/m}^3$$

$$T = 4.4 \times 10^3 \text{ }^\circ\text{K}$$

$$p_p = 1.7 \times 10^4 \text{ newtons/m}^2$$

$$\gamma = 1.16$$

$$Z = 1.02$$

$$a = 1.24 \times 10^3 \text{ m/s}$$

$$M = 1.6$$

The results of measurements of velocity during various runs show velocities between 6000 and 6850 meters per second with uncertainties of about 8 percent. The uncertainties were determined by having several persons make independent determinations of the velocity from the photographs, and from measurements made between the various frames in a given sequence.

The electrical power input into the arc heater and into the accelerator were measured for each run. The energy in the gas at the accelerator entrance is known from measurement of the energy loss to the cooling water of the arc heater and the nozzle. If the voltage drops estimated at the electrode sheaths are considered, then the energy added to the gas stream can be approximately determined. At the accelerator entrance,

$$h = 0.6 \times 10^7 \text{ joules/kgm}$$

$$\frac{u^2}{2} = 0.20 \times 10^7 \text{ joules/kgm}$$

The accelerator adds,

$$\Delta h = 1.6 \times 10^7 \text{ joules/kgm}$$

$$\Delta \frac{u^2}{2} = 1.6 \times 10^7 \text{ joules/kgm}$$

At the accelerator exit,

$$h = 2.2 \times 10^7 \text{ joules/kgm}$$

$$\frac{u^2}{2} = 1.8 \times 10^7 \text{ joules/kgm}$$

The calculated thrust of the accelerator is 20 newtons (4.5 lb).

The pitot tube used to measure stagnation pressure at the accelerator exit could not be used while velocity measurements were being made. The pitot pressure readings were consistent enough, however, that they can be used for the runs where velocity measurements were made. The measured pitot readings are  $2.1 \times 10^4$  newtons/m<sup>2</sup> (0.21 atm) with the accelerator off and  $7.6 \times 10^4$  newtons/m<sup>2</sup> (0.75 atm) when the accelerator is operating.

The shock-wave standoff distance from the pitot tube was measured and found to be 0.20 of the radius of the hemispherical end of the pitot tube. A calculation of the standoff distance, using the real-gas thermodynamic properties of nitrogen, was kindly made for us by personnel of the Ames Research Center of the NASA (ref. 2). This calculation yielded a standoff distance of 0.10 radius for the free-stream conditions of 0.067 atmosphere static pressure and 6000° K static temperature. The reason for the discrepancy is not known, but it may be that our estimate of the temperature is too low.

## 8. FUTURE ACCELERATORS

The present accelerator, though limited in running time, serves well during this phase of the research program. To overcome the disadvantage of limited running time, a water-cooled version of it has been designed and constructed. It contains 24 pairs of independently water-cooled copper electrodes and water-cooled sidewalls of copper which will be coated with various types of insulating materials to determine which is most satisfactory.

We are also proceeding with the design of an accelerator to give exit velocities of at least 12,000 meters per second at a density of  $3 \times 10^{-4}$  kg/m<sup>3</sup>. The accelerator will utilize an expanding channel of 2 by 2 inches cross section at the entrance and 4 by 4 inches or more at the exit, and will be 18 inches long. It will be operated from a 10-megawatt d-c supply and a second 10-megawatt d-c supply will power the arc heater.

# SYMBOLS

(Rationalized System of Units, mksck)

a	speed of sound, m/sec
B	magnetic induction, webers/m <sup>2</sup>
e	charge on electron, coulombs
E	electric field strength, volts/m
h	enthalpy, joules/kg
j	current density, amp/m <sup>2</sup>
l	distance across accelerator channel perpendicular to B field, m
$\dot{m}$	mass flow rate, kg/s
$m_{N_2}$	mass of nitrogen molecule, kg
M	Mach number, $u/a$
n	number density, particles/m <sup>3</sup>
p	pressure, newtons/m <sup>2</sup>
S	entropy, joules/kg-°K
T	temperature, °K
u	velocity, m/s
V	potential difference, volts
Z	compressibility factor
$\alpha$	degree of ionization

$$\gamma \equiv \left( \frac{\partial \ln p}{\partial \ln \rho} \right)_S$$

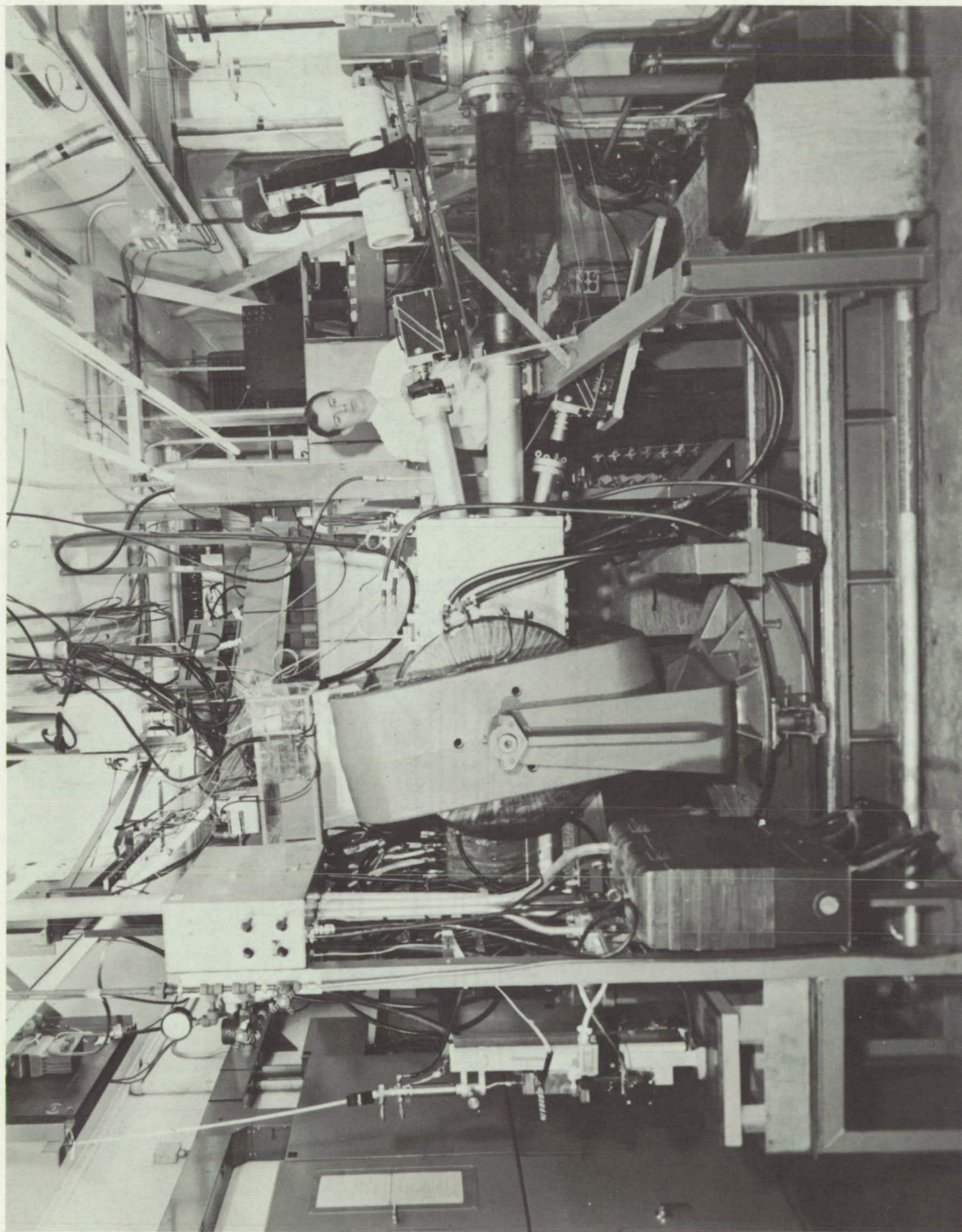
$\rho$	mass density, kg/m <sup>3</sup>
$\sigma$	scalar electrical conductivity, mho/m

Subscripts:

e	electron
n	neutral particles
P	pitot
t	total, stagnation
x	component in x-direction
y	component in y-direction
z	component in z-direction

## REFERENCES

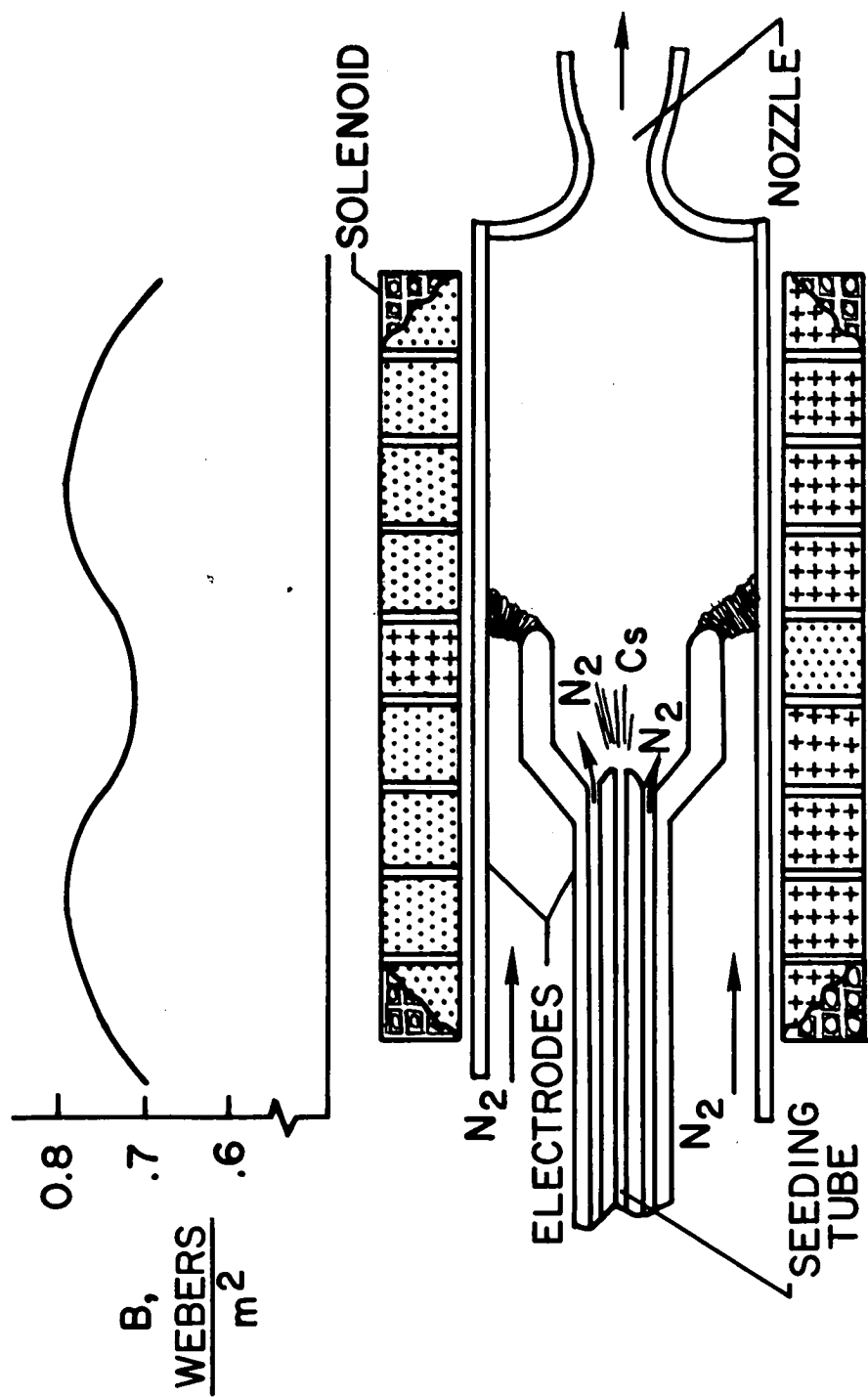
1. Wood, G. P., Carter, A. F., Sabol, A. P., McFarland, D. R., and Weaver, W. R.: Research on Linear Crossed-Field Steady-Flow D-C Plasma Accelerators at Langley Research Center, NASA. Presented at the AGARD Specialists' Meeting on Arc Heaters and MHD Accelerators for Aerodynamic Purposes. Rhode-Saint-Genèse, Belgium, September 21-23, 1964.
2. Lomax, Harvard: Private communication.



NASA

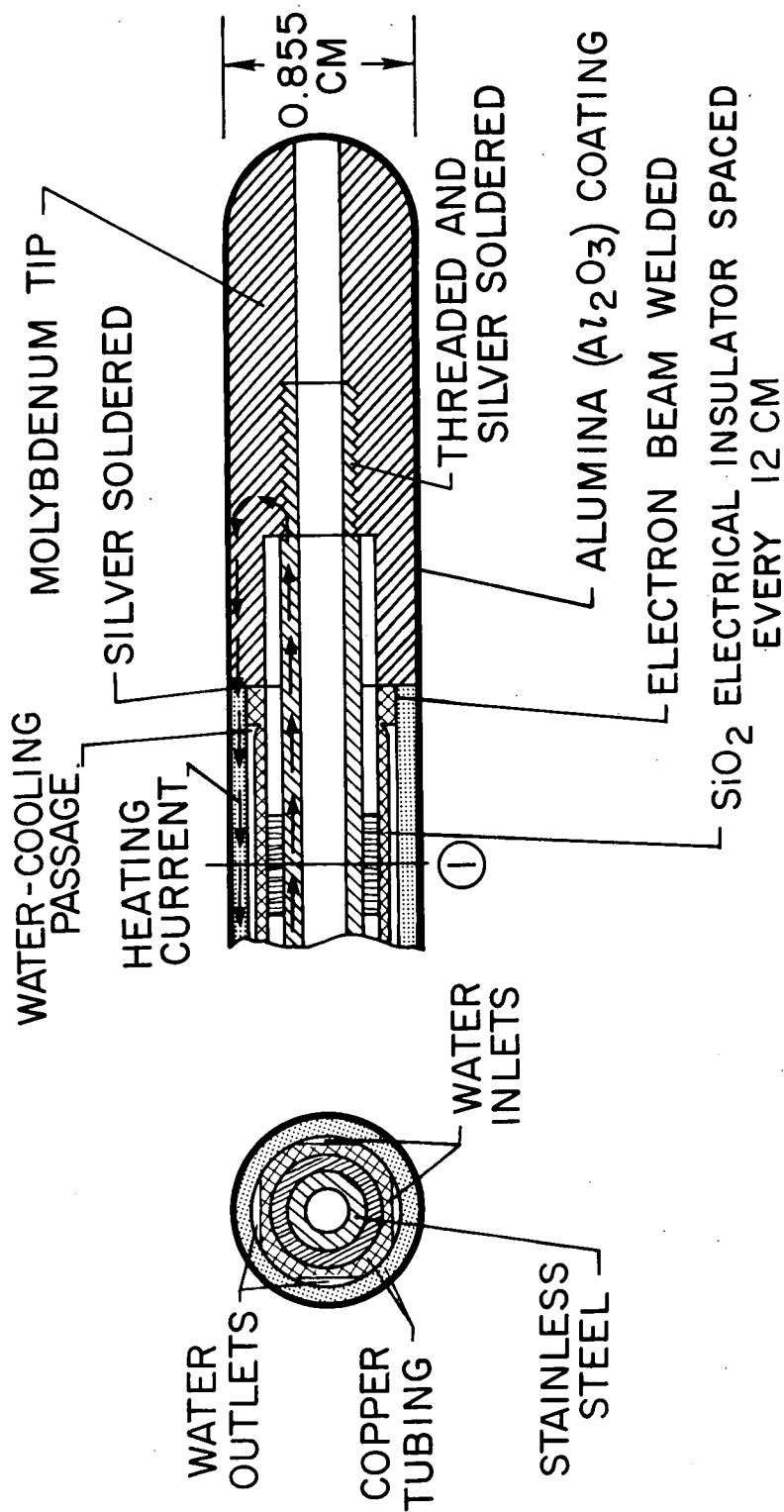
Figure 1.- Photograph of 1-inch-square accelerator installation.





NASA

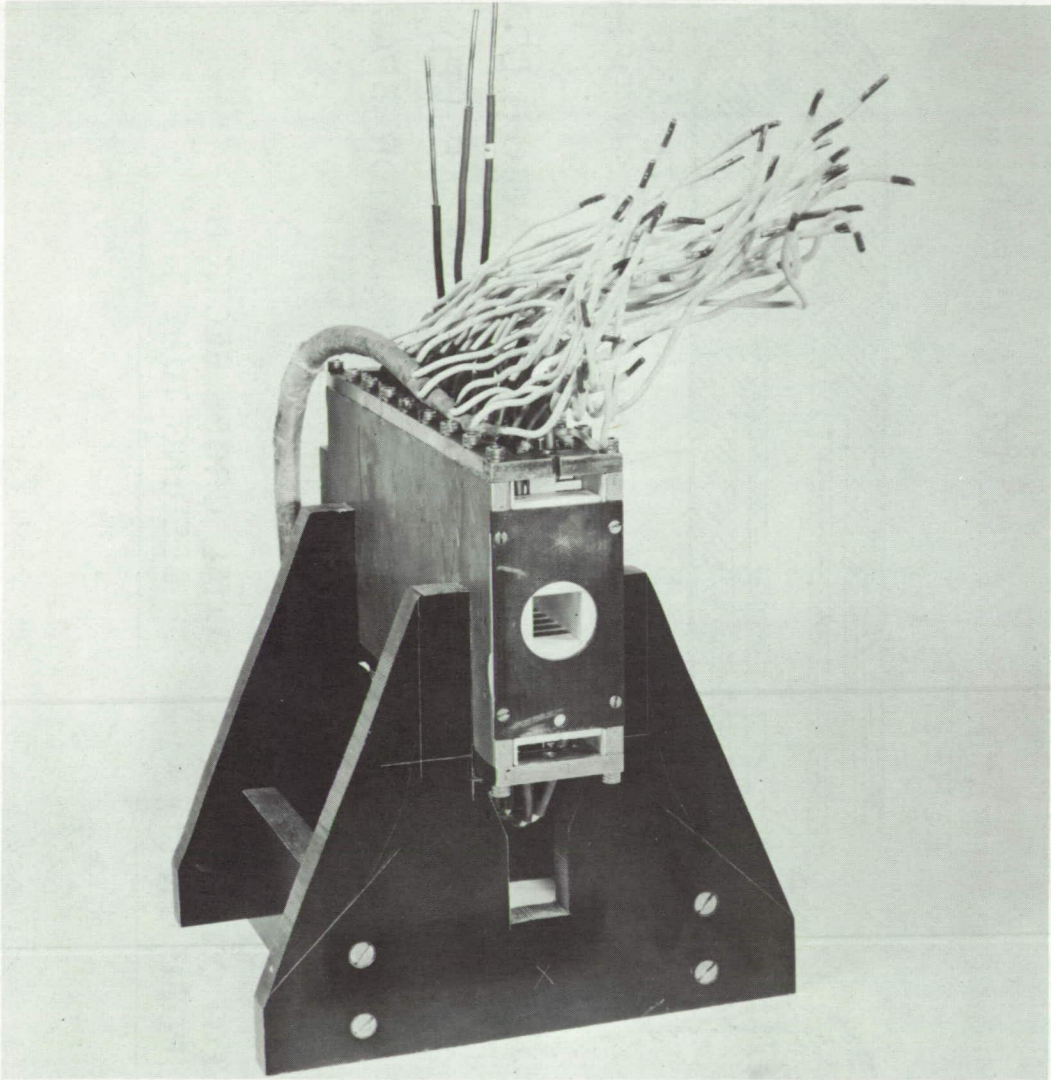
Figure 2.- Schematic diagram of arc heater and variation of magnetic induction.



CROSS SECTION  
OF TUBE AT POSITION ①

AXIAL CROSS SECTION  
OF SEEDING TUBE TIP

Figure 3.- Design of seeding tube.



NASA

Figure 4.- Assembled 1-inch-square accelerator.

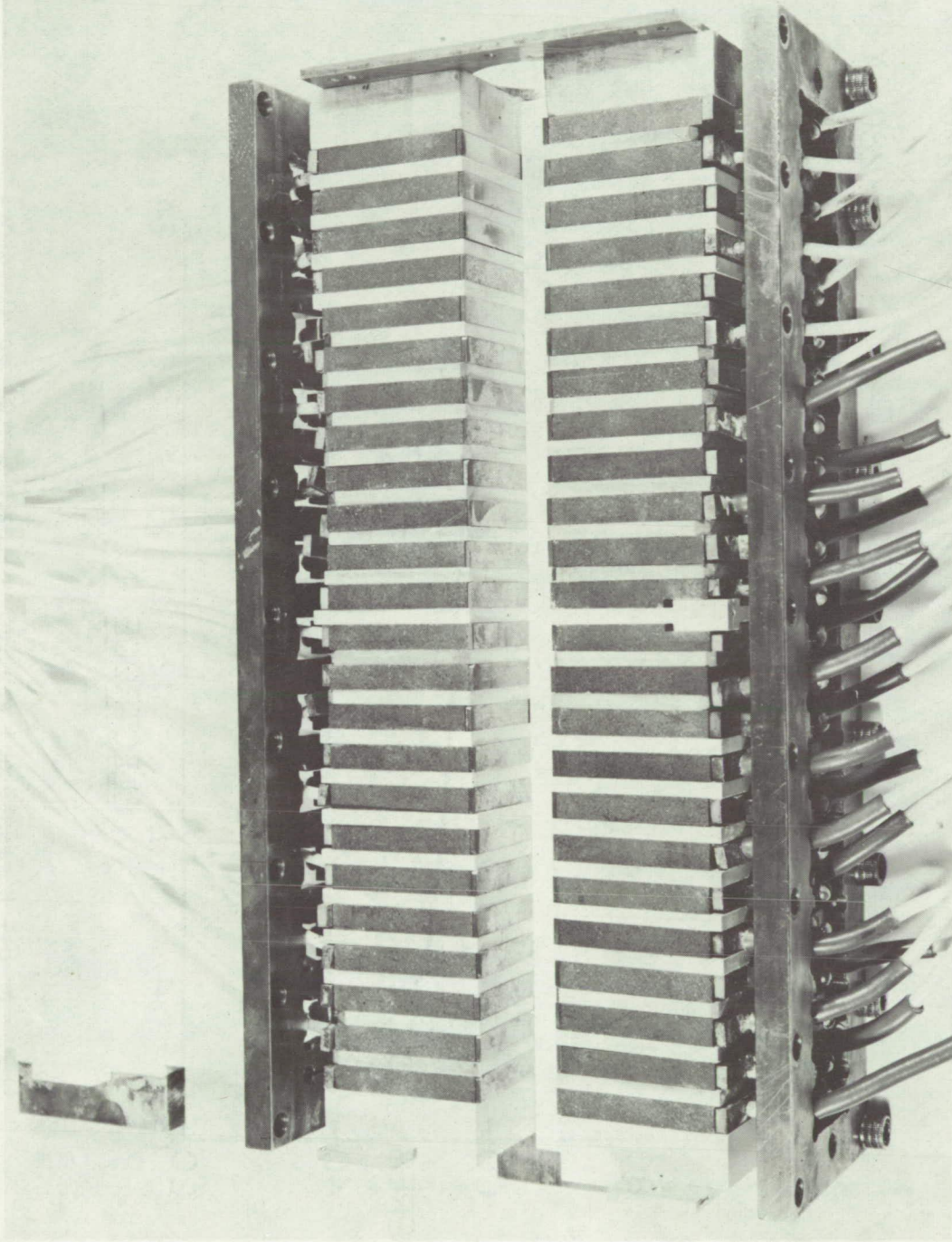
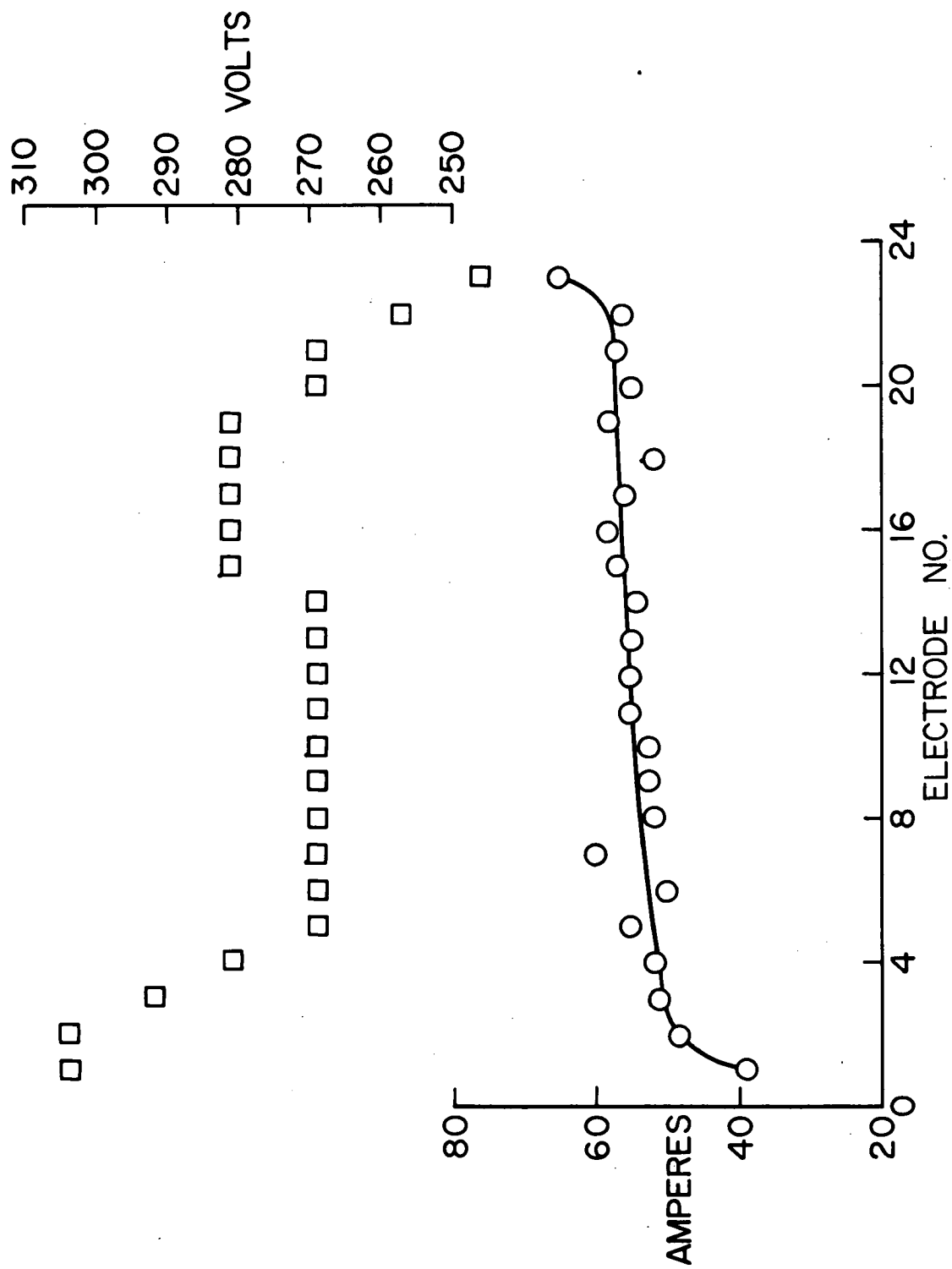


Figure 5.- Accelerator with sidewall removed.



NASA

Figure 6.- Currents and applied voltages across accelerator.



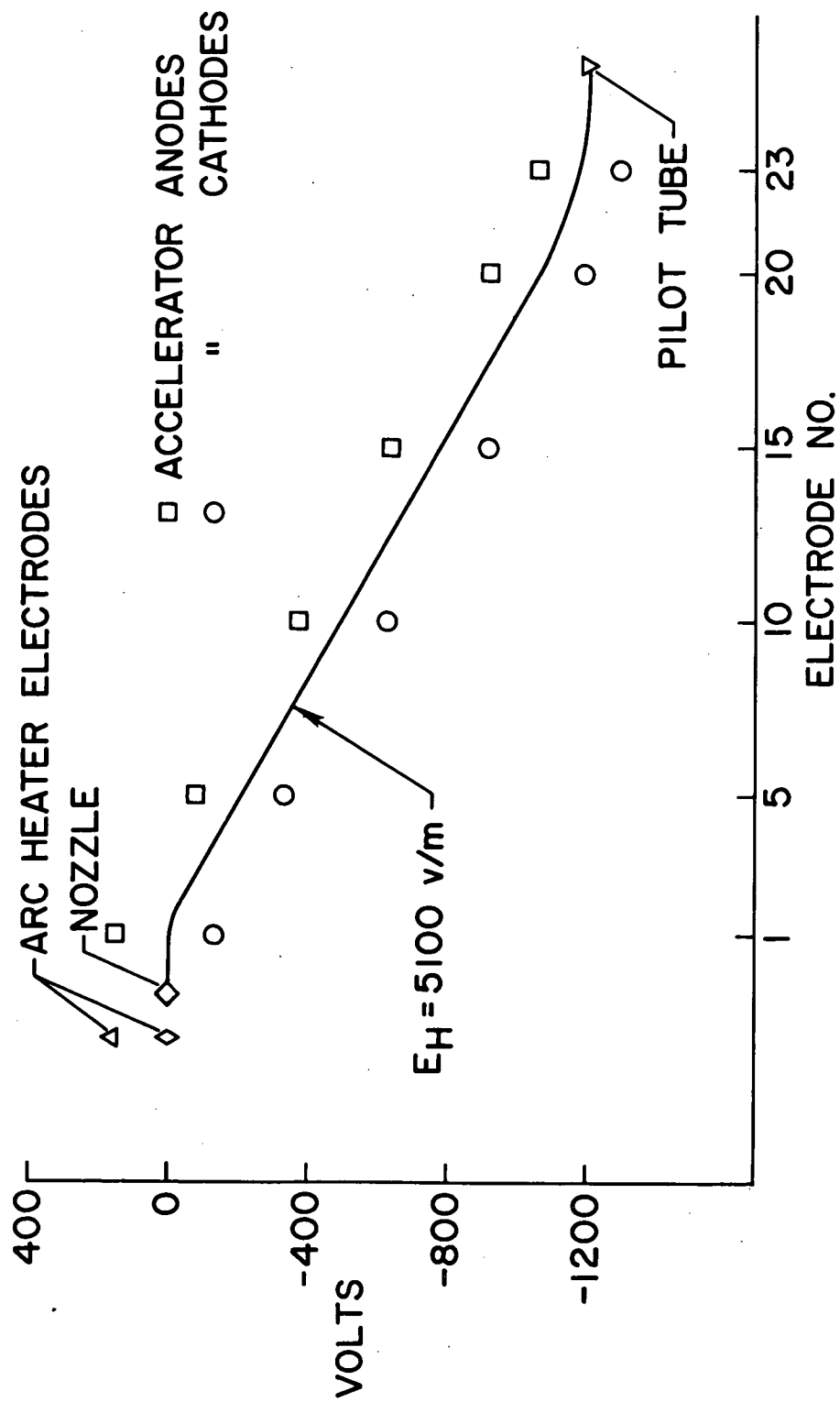


Figure 7.- Floating potential distribution in arc heater, nozzle, and accelerator.

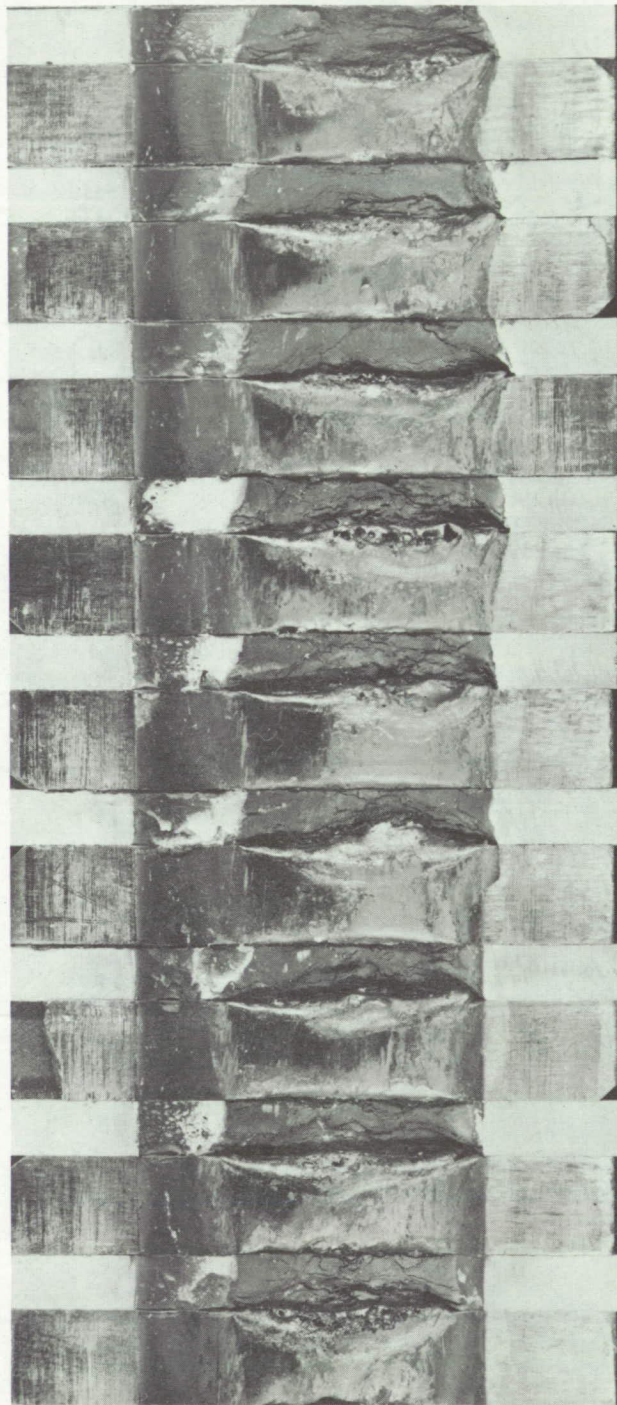


Figure 8.- Erosion of 1/16-inch-thick anodes.

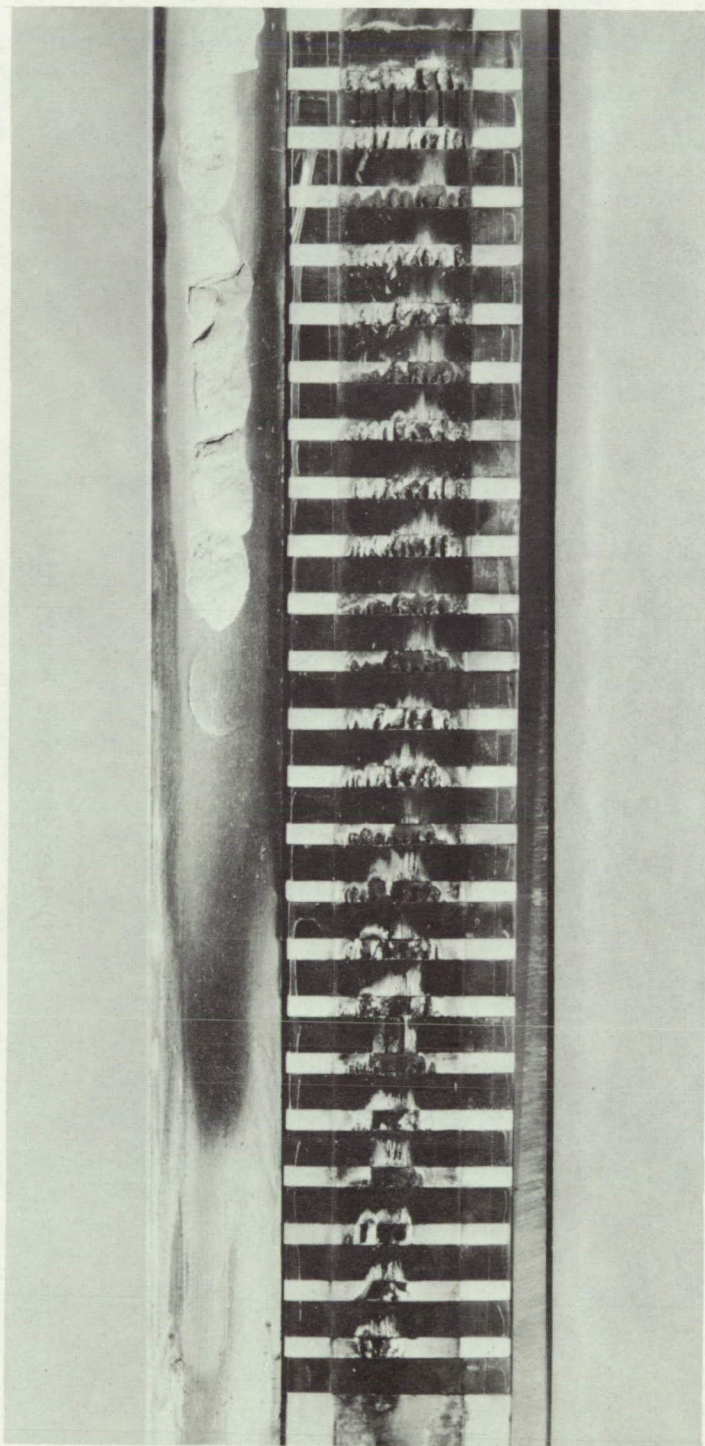
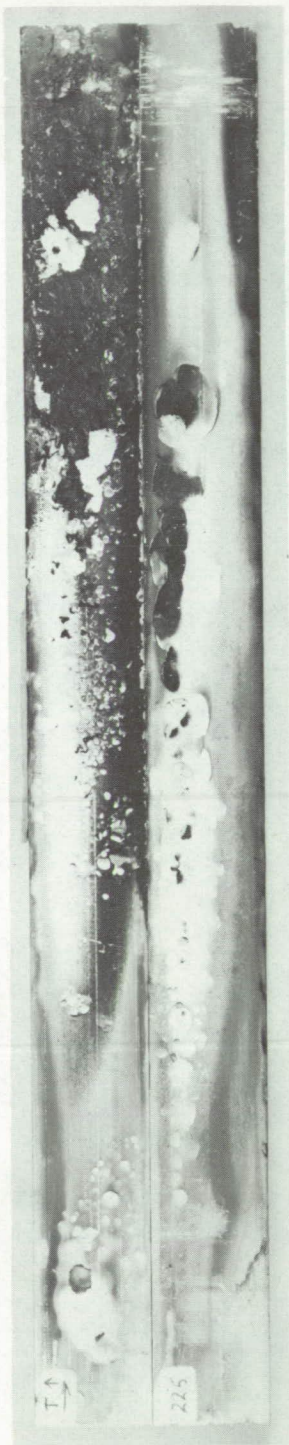
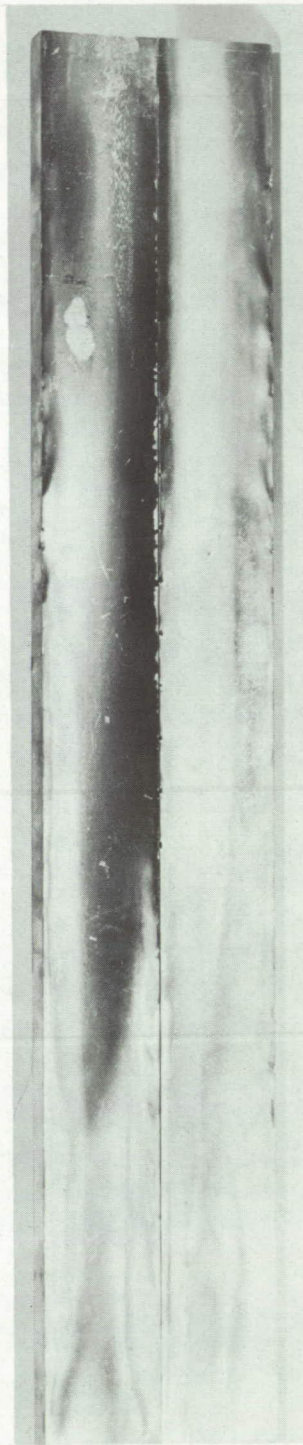


Figure 9.- Erosion of 1/4-inch-thick anodes.





(a) Boron nitride.



(b) New improved boron nitride.

Figure 10.- Sidewalls made of boron nitride.

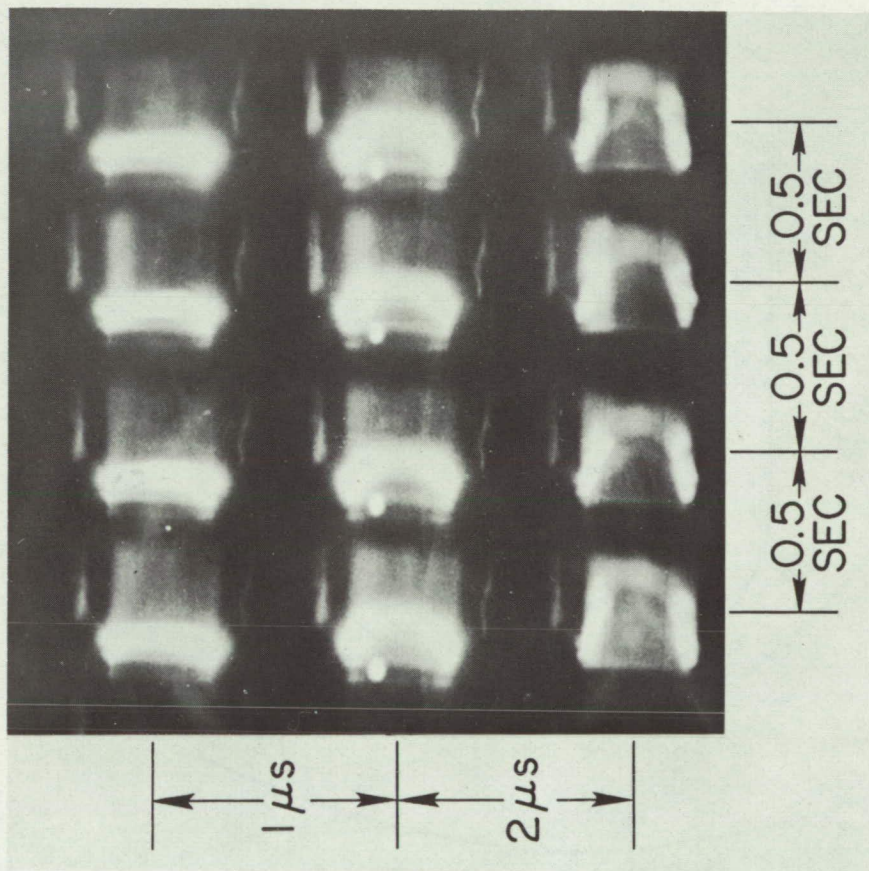
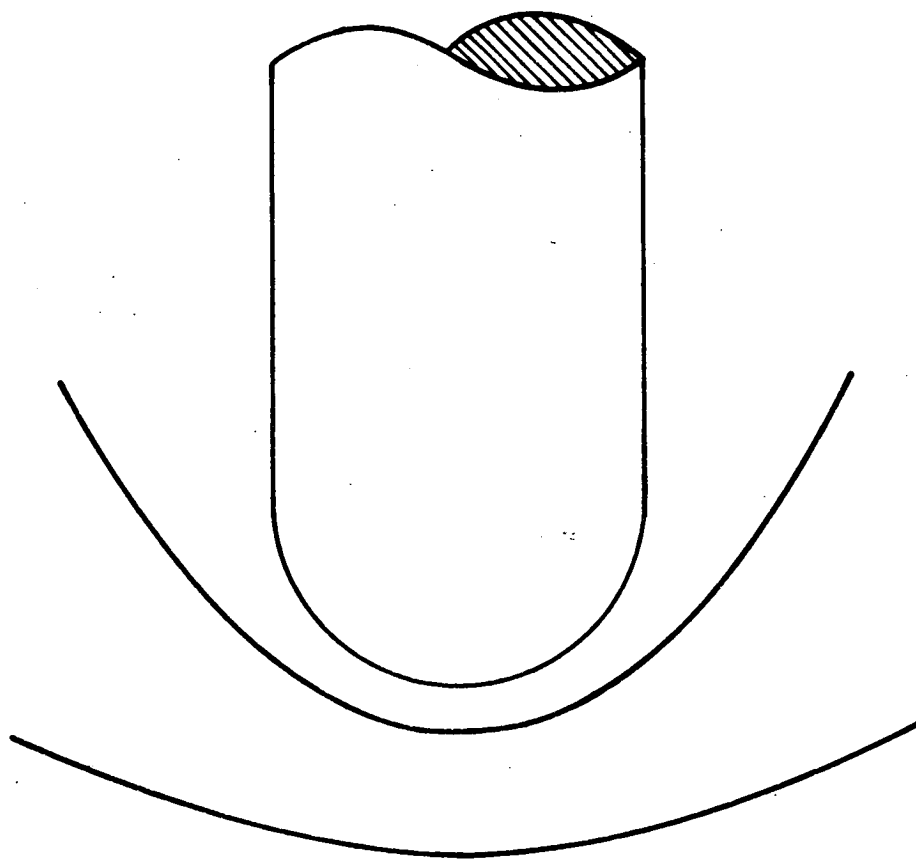


Figure 11.- Image converter camera pictures of luminous gas from spark.



NASA

Figure 12.- Bow shock waves with accelerator off and on (from photographs).